Received: 3 October 2021 | Revised: 23 March 2022 | Accepted: 22 May 2022

DOI: 10.1111/jre.13022

Journal of PERIODONTAL RESEARCH WILEY

ORIGINAL ARTICLE

LiCl-induced immunomodulatory periodontal regeneration via the activation of the Wnt/β-catenin signaling pathway

Xiumei Zheng[1,2] | Shengfang Wang[3] | Lan Xiao[2,3] | Pingping Han[2,4] | Kunke Xie[5] | Saso Ivanovski[2,4] | Yin Xiao[2,3,5] | Yinghong Zhou[2,4,5]

[1]Xiamen Key Laboratory of Stomatological Disease Diagnosis and Treatment, Stomatological Hospital of Xiamen Medical College, Xiamen, China

[2]The Australia-China Centre for Tissue Engineering and Regenerative Medicine (ACCTERM), Queensland University of Technology, Brisbane, Queensland, Australia

[3]School of Mechanical, Medical and Process Engineering, Centre for Biomedical Technologies, Queensland University of Technology, Brisbane, Queensland, Australia

[4]School of Dentistry, Faculty of Health and Behavioural Sciences, The University of Queensland, Brisbane, Queensland, Australia

[5]Guangzhou Key Laboratory of Basic and Applied Research of Oral Regenerative Medicine, Affiliated Stomatology Hospital of Guangzhou Medical University, Guangzhou, China

Correspondence
Yin Xiao and Yinghong Zhou, Guangzhou Key Laboratory of Basic and Applied Research of Oral Regenerative Medicine, Affiliated Stomatology Hospital of Guangzhou Medical University, Guangzhou, Guangdong 510182, China.
Emails: yin.xiao@qut.edu.au ; yinghong.zhou@uq.edu.au

Funding information
Australian Dental Research Foundation; Young Scientists Fund; National Natural Science Foundation of China; National Health and Medical Research Council

Abstract

Background: Growing evidence suggests that excessive inflammation hampers the regenerative capacity of periodontal ligament cells (PDLCs) and that activation of the Wnt/β-catenin pathway is crucial in suppressing immune dysregulation.

Objective: This study aimed to establish the role of the Wnt/β-catenin in regulating the immune microenvironment and its subsequent impact on periodontal regeneration.

Methods: Lithium chloride (LiCl, Wnt activator) was administered daily into the standard periodontal defects created in 12-week-old Lewis rats. Harvested at 1-week and 2-week post-surgery, samples were then subjected to histological and immunohistochemical evaluation of macrophage distribution and phenotype (pro-inflammatory M1 and anti-inflammatory M2). A murine macrophage cell line, RAW 264.7, was stimulated with LiCl to activate Wnt/β-catenin. Following treatment with the conditioned medium derived from the LiCl-activated macrophages, the expression of bone- and cementum-related markers of the PDLCs was determined. The involvement of Wnt/β-catenin in the immunoregulation and autophagic activity was further investigated with the addition of cardamonin, a commercially available Wnt inhibitor.

Results: A significantly increased number of macrophages were detected around the defects during early healing upon receiving the Wnt/β-catenin signaling cue. The defect sites in week 2 exhibited fewer M1 and more M2 macrophages along with an enhanced regeneration of alveolar bone and cementum in the Wnt/β-catenin activation group. LiCl-induced immunomodulatory effect was accompanied with the activation Wnt/β-catenin signaling, which was suppressed in the presence of Wnt inhibitor. Exposure to LiCl could induce autophagy in a dose-dependent manner, thus maintaining macrophages in a regulatory state. The expression level of bone- and cementum-related markers was significantly elevated in PDLCs stimulated with LiCl-activated macrophages.

Conclusion: The application of Wnt activator LiCl facilitates the recruitment of macrophages to defect sites and regulates their phenotypic switching in favor of periodontal regeneration. Suppression of Wnt/β-catenin pathway could attenuate the LiCl-induced immunomodulatory effect. Taken together, the Wnt/β-catenin pathway may be targeted for therapeutic interventions in periodontal diseases.

KEYWORDS
immunomodulation, inflammation, macrophages, periodontal regeneration

1 | INTRODUCTION

Periodontitis is a common chronic inflammatory disease characterized by the destruction of the supporting structures of the teeth, including periodontal ligament (PDL), cementum, and alveolar bone.[1] It is a major cause of tooth loss, resulting in tremendous adverse esthetic and functional outcomes. Periodontitis represents a collection of complex diseases involving interactions between the host immune systems, periodontal microbiota and modifying environmental and genetic factors.[2] This immune dysregulation is the result of an over-activated immunoinflammatory response to the microbial biofilm (dental plaque) and leads to the destruction of periodontal tissues by a chronic local immune response.[3] Current knowledge of periodontal diseases in terms of the etiology and pathology identifies the value of host modulation therapy as a key treatment strategy for managing periodontitis.

Macrophages, the major effector cells of the innate immune system, are crucial for effective host defense against pathogenic microorganisms in periodontal tissues.[4] Macrophages function as control switches of the immune system and provide a balance between pro- and anti-inflammatory responses by developing broadly into the two major subsets of classically activated pro-inflammatory M1 or alternatively activated anti-inflammatory M2. When properly controlled, M1 macrophages effectively destroy invading pathogens and foreign materials. However, when M1 activation becomes excessive or uncontrolled, these cells can release cytotoxic mediators that damage tissues. The activity of M1 macrophages is countered by M2 macrophages, which release anti-inflammatory cytokines involved in tissue repair. The balance in the production of mediators by these two macrophage subpopulations ultimately determines the tissue response.[5]

The Wnt/β-catenin signaling is an evolutionarily conserved pathway with a key role in embryogenesis, cell differentiation, stem cell maintenance, and renewal.[6] When the canonical Wnt/β-catenin signaling pathway is activated, β-catenin accumulates in the cytoplasm and nucleus to interact with TCF/LEF transcription factors, enhancing the expression of specific downstream genes.[7] Stimulation of macrophages with conserved microbial structures (such as LPS) can activate the NF-κB pathway, induce pro-inflammatory cytokines (such as TNF-α and IL-12), and reduce Axin 2 expression.[8] However, activation of canonical Wnt signaling inhibits the NF-κB regulator GSK3β and diminishes the expression of TNF-α and other pro-inflammatory cytokines.[9] Lithium chloride (LiCl) is an FDA approved drug that can activate the Wnt/β-catenin pathway by preventing β-catenin phosphorylation.[10] Owing to the regulatory role of the Wnt/β-catenin signaling pathway in immune response, LiCl has been reported to effectively regulate inflammation,[11–14] an effect beneficial for tissue regeneration (e.g., skin and bone).[12,13] Furthermore, LiCl has been reported to suppress the inflammatory response of monocytes (macrophage precursors), which is achieved through the activation of autophagy, an indispensable homeostatic cellular process with demonstrated anti-inflammatory capacity.[15] Therefore, LiCl has been proposed as a therapeutic agent in periodontal diseases, capable of promoting the transition of inflammatory microenvironment to a reparative state, thereby facilitating the regeneration of periodontal tissues.

This study tested the hypothesis that LiCl-mediated Wnt activation can modulate macrophage phenotypic changes and autophagic activities to resolve periodontal tissue inflammation and promote regeneration. As such, it highlighted the emerging interest in immunomodulatory therapeutics and established a molecular basis to develop innovative approaches to manage periodontal diseases.

2 | MATERIALS AND METHODS

2.1 | Cell culture

Human research ethics (No. 1900000941) approval was obtained from the Office of Research Ethics and Integrity (OREI), Queensland University of Technology (QUT). The PDLCs used in this study were harvested from caries-free and periodontally healthy premolars extracted for orthodontic treatment purposes from six donors, who provided full informed consent. The periodontal ligament tissues were gently dissected from the mid-1/3 of the root surface, trimmed down to fine pieces, and rinsed with phosphate-buffered saline (PBS).[16] The tissue explants were transferred to a primary culture dish and incubated at 37°C and 5% CO_2 in low-glucose Dulbecco's Modified Eagle Medium (DMEM; Life Technologies Australia Pty Ltd.) supplemented with 10% fetal bovine serum (FBS; Life Technologies Australia Pty Ltd.) and 50 U/ml penicillin/50 μg/ml streptomycin (P/S; Life Technologies Australia Pty Ltd.). The medium was changed twice a week, and the outgrown cells were passaged after reaching about 80% of confluence. Cells at passages 2–4 were used for subsequent experiments.

RAW 264.7 cells were expanded in DMEM with 5% FBS (heat-activated at 60°C for 30 min) and 1% P/S at 37°C in a humidified incubator. M1 pro-inflammatory phenotype was achieved by the supplementation of 1 μg/ml LPS to macrophage cultures. Various concentrations of lithium chloride (LiCl; 0, 2.5, and 5 mM) were also added to the medium to activate the Wnt/β-catenin signaling simultaneously. To further investigate the LiCl-induced Wnt activation and the subsequent immunomodulatory effect, 10 μM cardamonin (Wnt/β-catenin inhibitor) was added to the culture medium in the presence of 5 mM LiCl.[17] After 12-h stimulation, the preconditioned macrophages (1×10^7 cells grown in T75 flask) were washed with

PBS and then incubated with 10 ml of serum-free DMEM at 37°C for another 12 h. Macrophages were collected for phenotype characterization. The conditioned medium (CM) was collected and centrifuged at 1000×*g* for 5 min at 4°C to clear the supernatants and then mixed with osteogenic medium (DMEM supplemented with 10% FBS, 1% P/S, 10 mM β-glycerophosphate, 50 μM ascorbic acid, and 100 nM dexamethasone) for osteogenic differentiation of PDLCs.

2.2 | Real-time quantitative polymerase chain reaction (RT-qPCR)

Total RNA from preconditioned macrophages (for the detection of immune responses and autophagic activity) and macrophage CM-treated PDLCs (for the detection of osteogenic/cementogenic differentiation) was extracted using the TRIzol™ reagent (Life Technologies Australia Pty Ltd.). Complementary DNA was synthesized from 1 μg of total RNA using SensiFAST™ cDNA Synthesis Kit (Bioline Australia Pty Ltd.) according to manufacturer instructions. RT-qPCR primers (Table 1) were designed based on cDNA sequences from the NCBI sequence database. SYBR™ Green PCR Master Mix (Life Technologies Australia Pty Ltd.) was used for detection, and the target mRNA expressions were assayed on the QuantStudio™ 7 Flex Real-Time PCR System (Life Technologies Australia Pty Ltd.). Reactions were all conducted in triplicate for three independent experiments. Relative gene expression was normalized against the housekeeping genes *GAPDH* and *18s*.

TABLE 1 Primer sequences used for RT-qPCR

Fwd_*iNOS*	**5′-CAGAAGTGCAAAGTCTCAGACAT-3′**
Rev_*iNOS*	5′-GTCATCTTGTATTGTTGGGCT-3′
Fwd_*TNFα*	5′-CTGAACTTCGGGGTGATCGG-3′
Rev_*TNFα*	5′-GGCTTGTCACTCGAATTTTGAGA-3′
Fwd_*IL-8*	5′-CTCTTGGCAGCCTTCCTGATTT-3′
Rev_*IL-8*	5′-CTCTTGGCAGCCTTCCTGATTT-3′
Fwd_*CCR7*	5′-GGTGGTGGCTCTCCTTGTCA-3′
Rev_*CCR7*	5′-CGTGGTATTCTCGCCGATGT-3′
Fwd_*Arg1*	5′-CTGACCTATGTGTCATTTGG-3′
Rev_*Arg1*	5′-CATCTGGGAACTTTCCTTTC-3′
Fwd_*IL-10*	5′-CAGGACTTTAAGGGTTACTTG-3′
Rev_*IL-10*	5′-ATTTTCACAGGGGAGAAATC-3′
Fwd_*TGF-β*	5′-GGCCCAGCATCTGCAAAG-3′
Rev_*TGF-β*	5′-GGTCCTTGCGGAAGTCAATG-3′
Fwd_*CD206*	5′-AAATGATGAGCTGTGGATTG-3′
Rev_*CD206*	5′-CCATCCTTGCCTTTCATAAC-3′
Fwd_*CD163*	5′-AGTCTGCTCACGATACATAG-3′
Rev_*CD163*	5′-TCCTTCTGGAATAGATTGGG-3′
Fwd_*Runx2*	5′-AGGGACTATGGCGTCAAACA-3′
Rev_*Runx2*	5′-GGCTCACGTCGCTCATCTT-3′
Fwd_*OCN*	5′-ACCTAGCAGACACCATGAGGAC-3′
Rev_*OCN*	5′-RGGGGACTGAGGCTCCAAG-3′
Fwd_*CAP*	5′-CTGCGCGCTGCACATGG-3′
Rev_*CAP*	5′-GCGATGTCGTAGAAGGTGAGCC-3′
Fwd_*CEMP1*	5′-GGGCACATCAAGCACTGACAG-3′
Rev_*CEMP1*	5′-CCCTTAGGAAGTGGCTGTCCAG-3′
Fwd_*GAPDH*	5′-TCAGCAATGCCTCCTGCAC-3′
Rev_*GAPDH*	5′-TCTGGGTGGCAGTGATGGC-3′
Fwd_*18s*	5′-CACCCGAGATTGAGCAATAACAGG-3′
Rev_*18s*	5′-ATCACGAATGGGGTTCAACGG-3′

2.3 | Western blotting

The whole cell lysates from LiCl-stimulated macrophages with or without the presence of cardamonin were collected for Western blotting detection, and protein concentration measurements were conducted using the BCA Protein Assay Kit (Life Technologies Australia Pty Ltd.). A total of 10 μg of protein from each sample were separated on SDS-PAGE gels and then transferred onto 0.45 μm nylon-supported nitrocellulose membranes followed by incubation with the Odyssey Blocking Buffer (1:5000; LI-COR Biotechnology, USA) for 1 h at room temperature. The membranes were incubated with specific primary antibodies against inducible nitric oxide synthase (iNOS, M1 macrophage marker; Thermo Fisher Scientific, PA1-036, rabbit anti-mouse, 1:1000), Arginase (M2 macrophage marker; Abcam, ab91279, rabbit anti-mouse, 1:1000), β-catenin (Wnt signaling downstream effector; Cell Signaling Technology, #9562, rabbit anti-mouse, 1:1000), autophagy protein 5 (Atg5, autophagosome-formation marker; Abcam, ab108327, rabbit anti-mouse, 1:1000) and Beclin-1 (autophagic activity marker; Cell Signaling, #3738, 1:1000, rabbit anti-mouse, 1:1000), microtubule-associated protein 1A/1B-light chain 3 (LC3A/B, autophagic activity marker; Cell Signaling Technology, 4108, rabbit anti-mouse, 1:1000), and α-Tubulin (Abcam, 1:2000) in PBS-diluted Odyssey Blocking Buffer overnight at 4°C. The membranes were then washed with PBS-Tween20 (0.1%) and incubated with IRDye® 800CW goat anti-rabbit IgG (H + L) or IRDye® 680RD goat anti-mouse IgG (H + L) (1:5000, LI-COR for 1 h at room temperature. The membranes were washed again 3× with PBS-Tween20 (0.1%), and the specific protein signals were visualized using the Odyssey® CLx Imaging System (LI-COR Biotechnology, USA). Quantification of band intensities was obtained using the ImageJ software, and representative Western blot images were displayed. The osteogenic activity of PDLCs treated by the LiCl-stimulated macrophages was also investigated using osteogenic antibodies alkaline phosphatase (ALP; Abcam, 1:1000), collagen type 1 (Col-1; Abcam, ab34710, 1:1000), and runt-related transcription factor 2 (Runx2; Cell Signaling, #12556, 1:1000).

2.4 | Immunofluorescence staining

LiCl-stimulated macrophages were fixed with 4% paraformaldehyde (PFA) for 15 min, permeabilized with 0.25% Triton X-100 for 10 min,

and blocked with 4% BSA for 1 h at room temperature, prior to incubation with rabbit polyclonal antibody against iNOS (Thermo Fisher Scientific, PA1-036, 1:100), Arginase (Abcam, ab91279, 1:100) and β-catenin (Cell Signaling Technology, #9562, 1:200) overnight at 4°C. Fluorescein isothiocyanate-conjugated goat anti-rabbit IgG (Sigma-Aldrich, Australia) was applied as the secondary antibody. Actin cytoskeletons were labeled by phalloidin and nuclei by DAPI. Samples were mounted on glass slides with ProLong Gold Antifade Mountant (Thermo Fisher Scientific, Australia), and images were visualized with the confocal laser scanning microscope (Nikon A1R Confocal).

2.5 | Monodansylcadaverine staining

The autofluorescent agent monodansylcadaverine (MDC) was used to detect autophagic vacuoles in LiCl-stimulated macrophages. After exposure to 0, 2.5, and 5 mM of LiCl for 1 h, macrophages were fixed with 4% PFA and stained with 20 μM MDC (Sigma-Aldrich) for 30 min at 37°C in the dark. After incubation, the cells were washed with PBS and the visualization of MDC staining was detected with the Nikon A1R Confocal, and the intracellular MDC intensity was quantified using the ImageJ software.

2.6 | Alizarin Red S staining

Mineral deposits were visualized with Alizarin Red S staining on the two-week osteogenic culture of PDLCs (pre-mixed with CM derived from activated macrophages). The cells were fixed in 4% paraformaldehyde (PFA) for 10 min at room temperature and then stained with 2% Alizarin Red S solution (pH adjusted to 4.1) for 20 min. Following the removal of the unincorporated excess dye with distilled water, the mineralized nodules were labeled as red spots. Representative images were then captured with the Nikon optical microscope. For quantification, the deposits bound to Alizarin Red were extracted with 50% acetic acid solution, which was then placed into 1.5-ml Eppendorf tubes and vortexed for 30 s, prior to NaOH being added to adjust the pH to 4.1. Triplicates of 100 μl were transferred to a 96-well plate, and the optical density was analyzed at a wavelength of 405 nm.

2.7 | Rat periodontal defect model

All animal procedures in this study were approved by the Queensland University of Technology Animal Ethics Committee (Approval No. 1100000141) and compliant with the Animal Research: Reporting of In Vivo Experiments (ARRIVE) guidelines. Twelve-week-old male Lewis rats (Animal Resources Centre, Australia) were randomly allocated into control group (PBS injection) and treatment group (LiCl injection). The animals were anaesthetized with 3% (w/v) isoflurane inhalation, followed by a subcutaneous injection of buprenorphine (0.005 mg/kg) and meloxicam (1 mg/kg), combined with a local injection of lignocaine (1 ml of 1% lignocaine/cm of tissue) at the incision site for analgesia. A rat periodontal defect model of 3 mm (length) × 2 mm (width) × 1 mm (depth) was created as previously reported[18] (Figure S1). Oral analgesics (Tramadol, 25 mg/L of drinking water) was used post-operatively to alleviate pain and discomfort. All animals were recovered on a heating pad and then housed in independent cages with a soft diet. LiCl was administered daily into the periodontal defect between the mandibular first and second molars and near the base of the interproximal gingival papillae at a dose of 149 mg/kg.[18,19] Local injection of PBS served as the vehicle control. The rats were sacrificed 7 and 14 days following surgery. Samples were then harvested for histological and immunohistochemical analysis ($n = 6$ for each group at each time point).

2.8 | Micro-computed tomography (μCT) scanning and histological and immunohistochemical analysis

The rat mandibles were fixed in 4% PFA at 4 °C for 24 h and transferred to PBS for μCT scanning (μCT40; SCANCO Medical AG, Brüttisellen, Switzerland) with high resolution of 12 μm, voltage of 45 kVp, and current of 177 mA. The three-dimensional (3D) images were reconstructed from scans created by the μCT system software. Through 3D reconstructed images, the bone volume fraction (BV/TV) was calculated and analyzed to evaluate the alveolar bone quantity. Following μCT analysis, all specimens were then rinsed with PBS and demineralized in 10% EDTA for 8 weeks at room temperature. After decalcification was completed, the specimens were embedded in paraffin and sectioned for histological and immunohistochemical analysis. Serial sections were stained with hematoxylin and eosin (H&E) for general observation. AZAN staining was performed to identify the newly formed cementum and periodontal ligament alignment. AZAN staining provides the optimal contrast, where cell nuclei are stained dark red with azocarmine and collagen stained blue with aniline blue. Histological images were captured with a Zeiss Axio Scope A1 Microscope.

Immunohistochemical staining was performed after dewaxing, hydration, and neutralization of endogenous peroxidase activity. Sections were then incubated with optimal dilutions of primary antibodies against CD68 (Abcam, ab125212, 1:100), iNOS (Thermo Fisher Scientific, PA1-036, 1:100), Arginase (Abcam, ab91279, 1:100), CAP (Santa Cruz Biotechnology, 1:200), and ALP (Abcam, ab5694, 1:200) overnight at 4°C, followed by incubation with a biotinylated universal secondary antibody (DAKO) for 15 min at room temperature, and then with HRP-conjugated streptavidin-biotin complex for another 15 min. Rabbit IgG isotype control antibody was used in place of the primary antibodies to evaluate non-specific staining. The antibody complexes were visualized with the addition of a buffered diaminobenzidine (DAB) substrate for 3 min. Mayer's hematoxylin was used for counterstaining.

2.9 | Statistical analysis

All data were analyzed using SPSS statistics software with results expressed as mean ± standard deviation. Statistical differences between groups were determined by one-way analysis of variance (ANOVA) with Bonferroni's post hoc test. A p-value <.05 was considered statistically significant.

3 | RESULTS

3.1 | Early periodontal defect healing involved macrophage infiltration and Wnt/β-catenin signaling activation

In the present study, we used a rat periodontal defect model to evaluate macrophage infiltration during periodontal regeneration. As shown in the H&E staining results (Figure S2), alveolar bone regeneration was observed from 1 week to 2 weeks after surgery. Obvious macrophage infiltration ($CD68^+$ cells, Figure S2) in the periodontal defect area could be observed in the early stage (1 week) of periodontal regeneration, while much fewer $CD68^+$ cells were found in the later stage (2 weeks), suggesting macrophage infiltration was most prominent at early time points. Interestingly, the level of Wnt/β-catenin signaling, as indicated by β-catenin staining, showed a similar trend (high in the early time point and low in the later time point, Figure S2) to CD68 expression, suggesting a possible association between macrophage infiltration and activation of the Wnt/β-catenin signaling pathway.

3.2 | LiCl-induced periodontal regeneration was associated with M2 polarization

The effect of LiCl on periodontal regeneration was further demonstrated in vivo. As shown in Figure 1, LiCl administration significantly induced periodontal hard tissue repair and well-organized periodontal ligament when compared to the PBS-administration controls, as indicated by the μCT, AZAN staining, and H&E staining results (Figure 1). Quantitative assessment of bone volume fraction (BV/TV) was shown in Figure S3, where a significantly higher BV/TV was found in the LiCl treatment group at both 1 and 2 weeks compared with the control group. The activation of Wnt/β-catenin signaling could be observed in the LiCl treatment group, in which the β-catenin expression was higher at both 1 and 2 weeks than that in the PBS-treated control. Local administration of LiCl for two weeks led to the infiltration of macrophages, and the major components were of M2 phenotype, as indicated by the IHC staining against Arginase. On the contrary, the M1 phenotype ($iNOS^+$ cells) was obviously suppressed by LiCl treatment, as compared to the PBS-treatment group.

3.3 | LiCl activated Wnt/β-catenin signaling and M2 polarization in vitro

Increasing concentrations of LiCl also led to significantly reduced M1 marker expressions (such as *iNOS*, *TNF-α*, and *CCR7*) and increased M2 marker expressions (such as *Arg-1*, *IL-10*, and *CD163*) dose-dependently as demonstrated by the RT-qPCR analysis (Figure 2A). The supplementation of LiCl activated Wnt/β-catenin signaling in macrophages as evidenced by the increased β-catenin protein expression (Figure 2B) and nuclear translocation (Figure 3C) in a dose- and time-dependent manner, regulating phenotypic switch of M1-to-M2 macrophages (Figure 2B). Immunofluorescent staining further demonstrated that the exposure to LiCl in a dose-dependent manner led to a reduction in the expression of the pro-inflammatory M1 marker iNOS (Figure 3A) along with a distinct increase in the anti-inflammatory M2 marker Arginase expression (Figure 3B). Suppressing the Wnt/β-catenin signaling with the supplementation of 10 μM cardamonin in the 5 mM LiCl-treated group led to a significant reduction in β-catenin protein expression (Figure 4B). The markedly increased M1 marker expressions along with decreased M2 marker expressions suggested that Wnt signaling inactivation contributed to macrophage phenotype switching from M2 to M1 (Figure 4A).

3.4 | LiCl induced autophagic activity in macrophages

LiCl treatment (high-dose) induced the mRNA levels of Atg5 and Atg7, two essential molecules for the induction of autophagy (Figure 5A). The protein levels of Atg5 and Beclin-1, as well as the transition from LC3-I to LC3-II (a hallmark of autophagy), were also induced in macrophages treated with LiCl, suggesting LiCl treatment could activate autophagic activity in macrophages (Figure 5B). MDC-positive puncta (sphere-like structures indicated by white arrowheads in Figure 5C) increased in LiCl-treated macrophages when compared to the control group, implying that LiCl treatment induces autophagosome formation in macrophages. On the contrary, the application of Wnt inhibitor diminished the LiCl-induced autophagic activity as demonstrated in the significantly lower mRNA and protein expression levels of autophagy markers (Figure 6).

3.5 | Li-activated macrophages mediated osteogenic/cementogenic differentiation of PDLCs

The conditioned medium derived from LiCl-activated macrophages further mediated the osteogenic and cementogenic differentiation of PDLCs as shown by the increased mRNA expression levels of osteogenic markers (Runx2 and OCN) and cementogenic markers (CAP and CEMP1) on day 3 and day 7 of differentiation, respectively

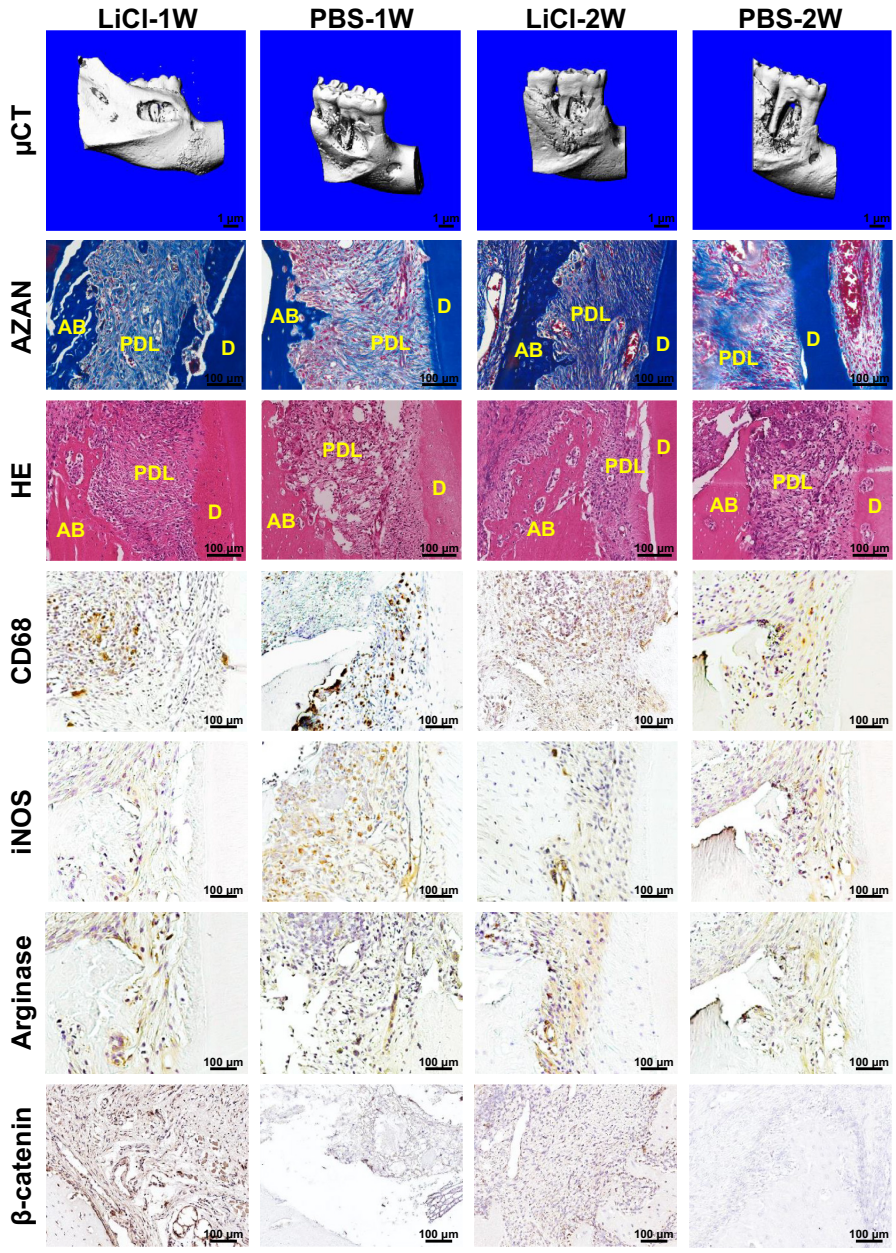

FIGURE 1 LiCl-induced periodontal regeneration was associated with M2 polarization. Representative images from μCT, AZAN staining, and H&E staining showed that LiCl administration significantly induced periodontal tissue repair compared with the PBS-administration controls. Immunohistochemical staining demonstrated the successful activation of Wnt/β-catenin signaling induced by LiCl administration, which further led to the infiltration of macrophages ($CD68^+$ cells) where the major components were of $Arginase^+$ M2 phenotype and the $iNOS^+$ M1 phenotype was obviously suppressed, at both 1 and 2 weeks as compared to the PBS-treatment group. AB, alveolar bone; D, dentin; PDL, periodontal ligament

(Figure 7A). This trend was further confirmed at the protein levels by the Western blot analysis (Figure 7B). More mineral depositions were found in LiCl-activated macrophage-derived conditioned medium-treated PDLCs in a dose-dependent manner, as demonstrated with Alizarin Red S staining (Figure 7C).

4 | DISCUSSION

Chronic inflammation is an underlying feature of highly prevalent diseases, including diabetes, inflammatory bowel disease, and periodontitis.[4] It is subclinical endotoxemia that has emerged as a common factor correlating with these diseases and potentially leading to chronic inflammation characterized by non-resolving inflammatory monocytes and macrophages.[20]

Periodontal therapy ultimately aims to establish a microenvironment that favors repopulation and differentiation of PDLCs, serving to reconstruct functionally oriented periodontal ligaments that insert into the alveolar bone on one side and cementum on the other.[21] As the major innate immune effector cells, macrophages are crucial for effective host defense against pathogenic microorganisms. Distorted immune responses as seen in some patients with periodontitis or other local and systemic diseases can, however, hamper the regenerative capacity of PDLCs and lead to periodontal tissue destruction.[22] Therefore, understanding the interaction of macrophages and PDLCs involved in periodontal tissue homeostasis is imperative, as it governs a microenvironment that may favor tissue repair after initial periodontal therapy (scaling and root planing) and, therefore, leading to the development of therapeutics to regenerate damaged periodontium.

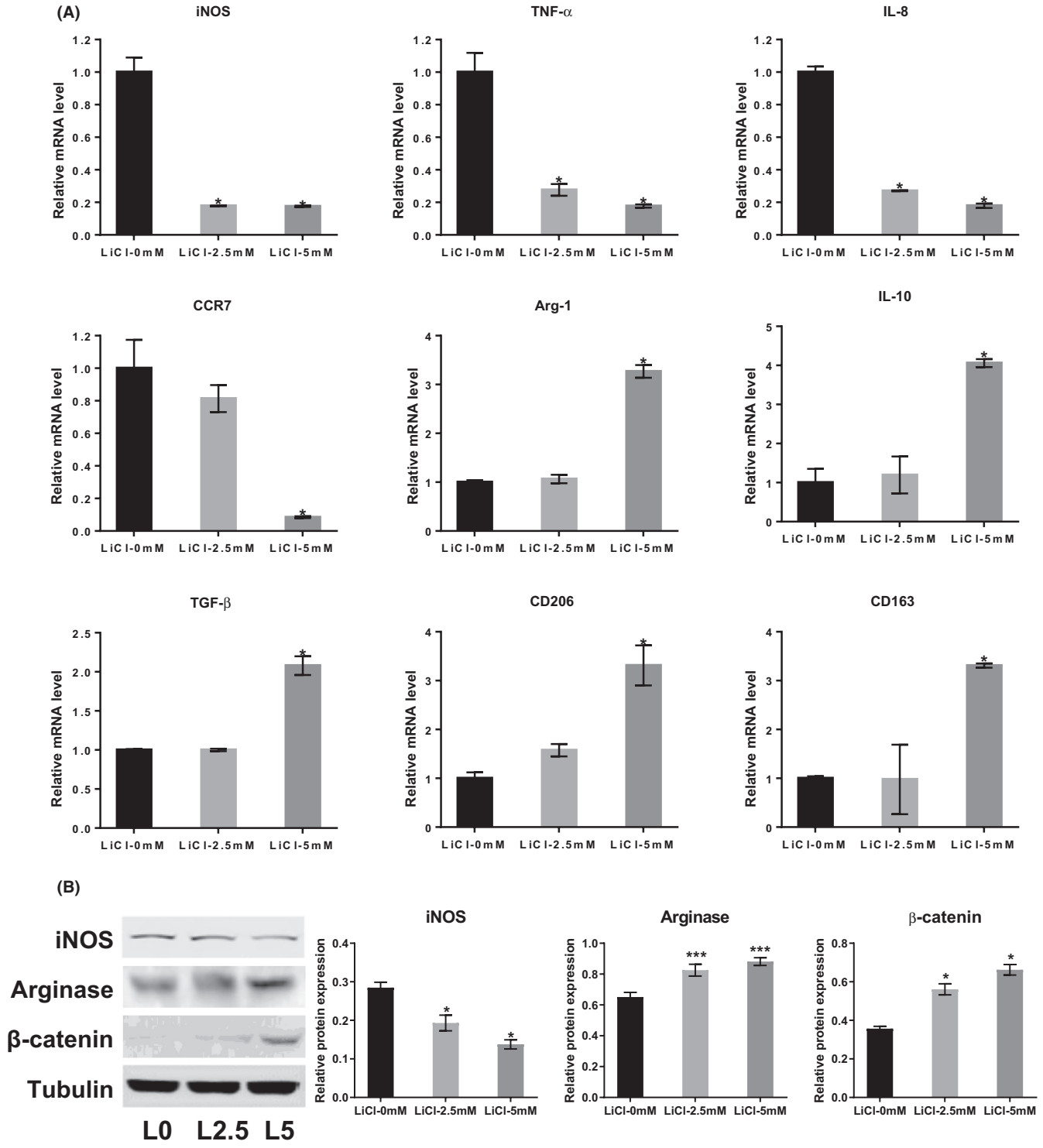

FIGURE 2 LiCl activated Wnt/β-catenin signaling and M2 polarization in vitro. (A) RT-qPCR analysis showed that the increasing concentrations of LiCl led to significantly reduced M1 marker expressions and increased M2 marker expressions dose-dependently. (B) Western blot analysis demonstrated a LiCl-induced Wnt/β-catenin signaling activation along with a down-regulation of the M1 (iNOS) and an upregulation of the M2 (Arginase) marker. The protein levels of β-catenin were also significantly increased after the LiCl treatment. Asterisk indicates significant difference (*$p < .05$; ***$p < .001$)

While several signaling pathways have been well characterized to induce inflammation, less is understood about the suppression and resolution mechanisms that control it. Studies have identified that the Wnt signaling pathway, particularly in innate immune cells, does play a critical role in regulating the resolution of inflammation.[23] In the canonical Wnt/β-catenin pathway, the binding of Wnt ligands to the Frizzled transmembrane receptors and to the low-density-lipoprotein-related protein co-receptors (LRP5/6) inhibits a

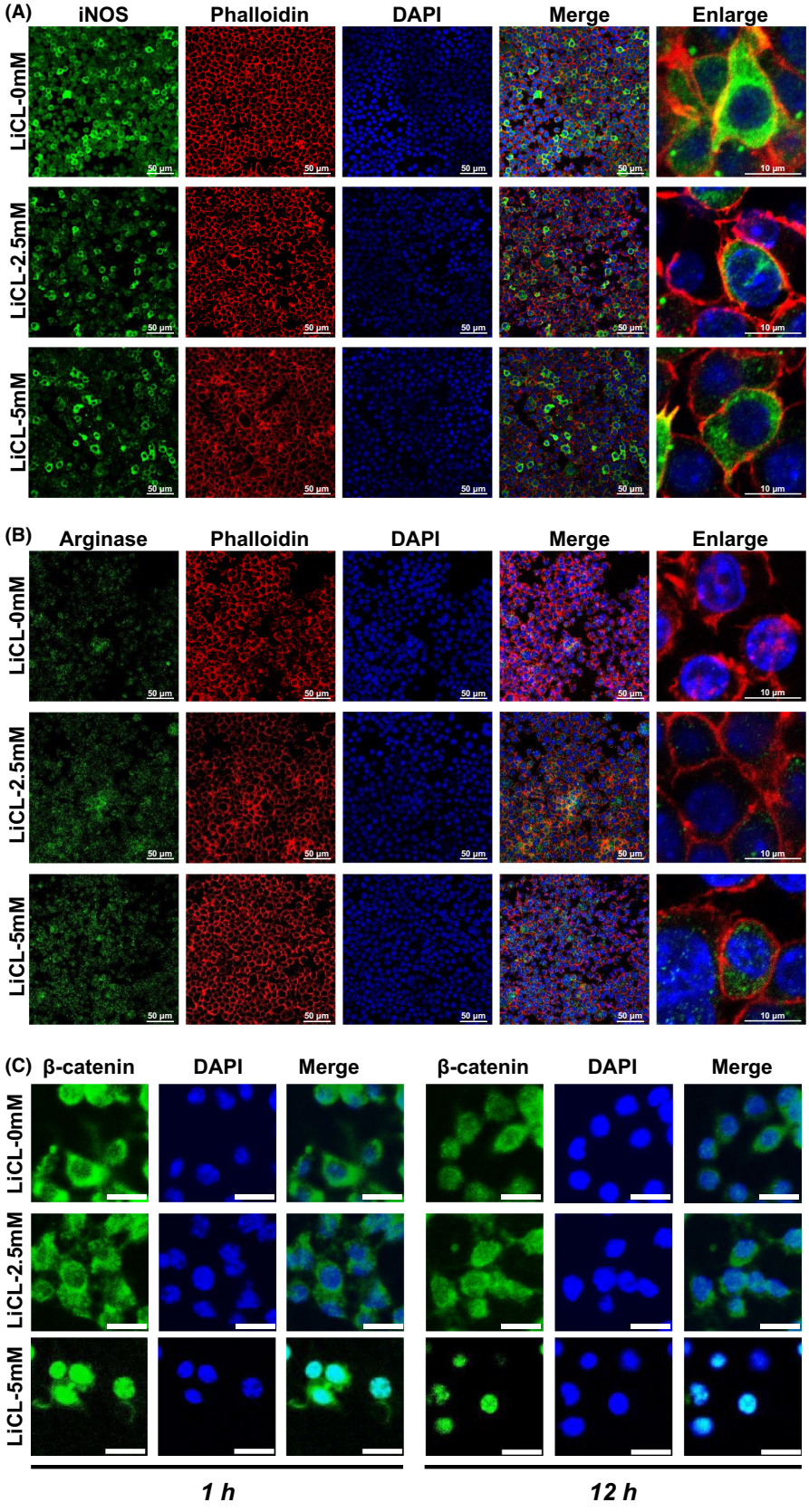

FIGURE 3 Immune response of macrophages to various concentrations of LiCl and β-catenin nuclear translocation. (A and B) Immunofluorescent staining demonstrated that the exposure to LiCl in a dose-dependent manner led to a reduction in the expression of pro-inflammatory M1 marker iNOS along with a distinct increase in the anti-inflammatory M2 marker Arginase expression. (C) In response to the Wnt stimulus, β-catenin was stabilized and translocated to the nucleus, where it exerted its function

protein complex responsible for degradation of the cytosolic effector protein β-catenin.[24,25] Following the inactivation of the β-catenin destruction complex, β-catenin translocates to the nucleus, where it associates with T-cell factor/lymphoid enhancer-binding factor (TCF/LEF) transcription factors.[26] The resulting complexes bind and regulate the promoter sequences of Wnt/β-catenin target genes.

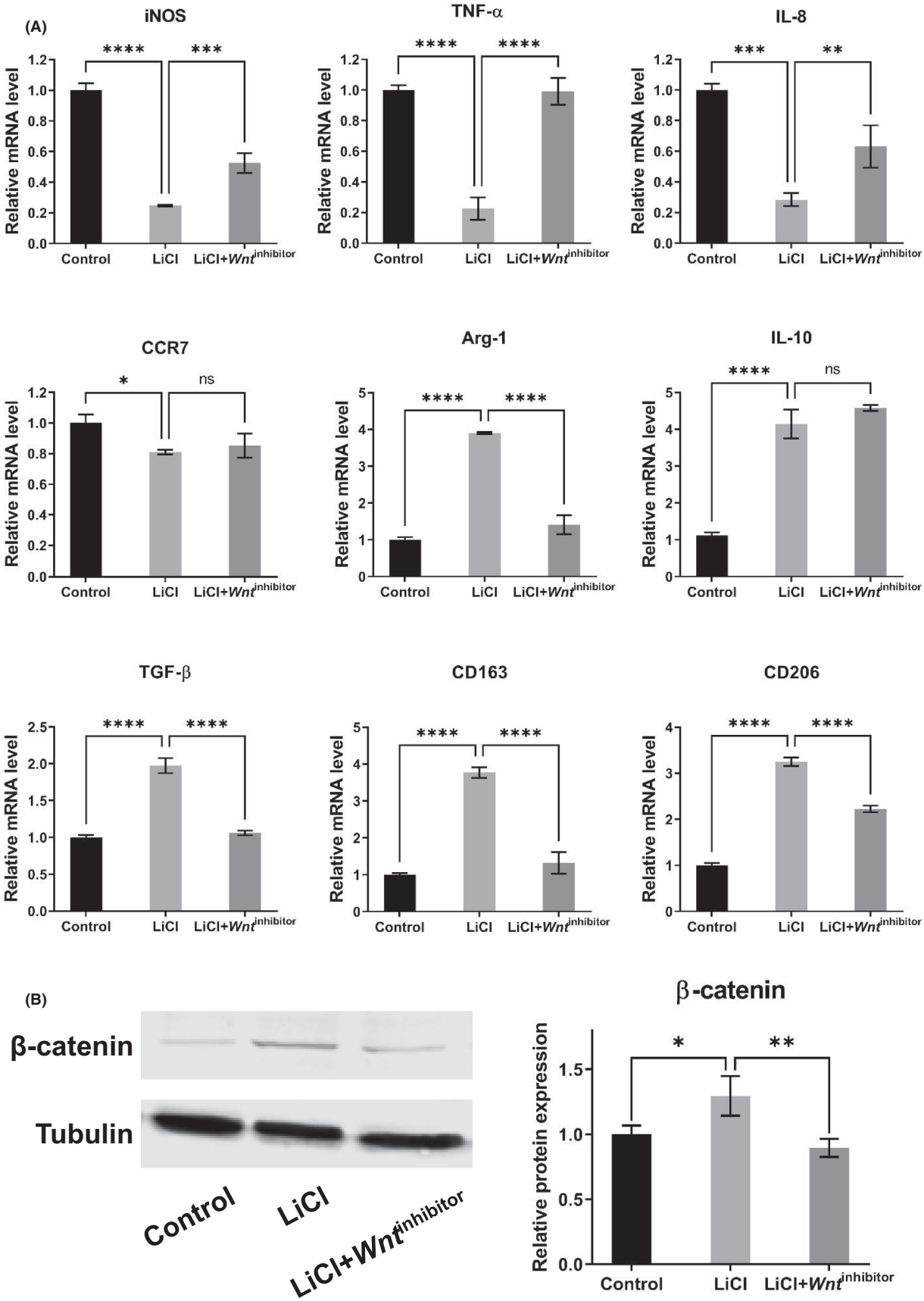

FIGURE 4 Suppressing the Wnt/β-catenin signaling with the supplementation of Wnt inhibitor (10 μM cardamonin) led to (A) markedly increased M1 marker expressions along with decreased M2 marker expressions, and (B) a significant reduction in β-catenin protein expression. Asterisk indicates significant difference (*$p < .05$; **$p < .01$; ***$p < .001$; ****$p < .0001$)

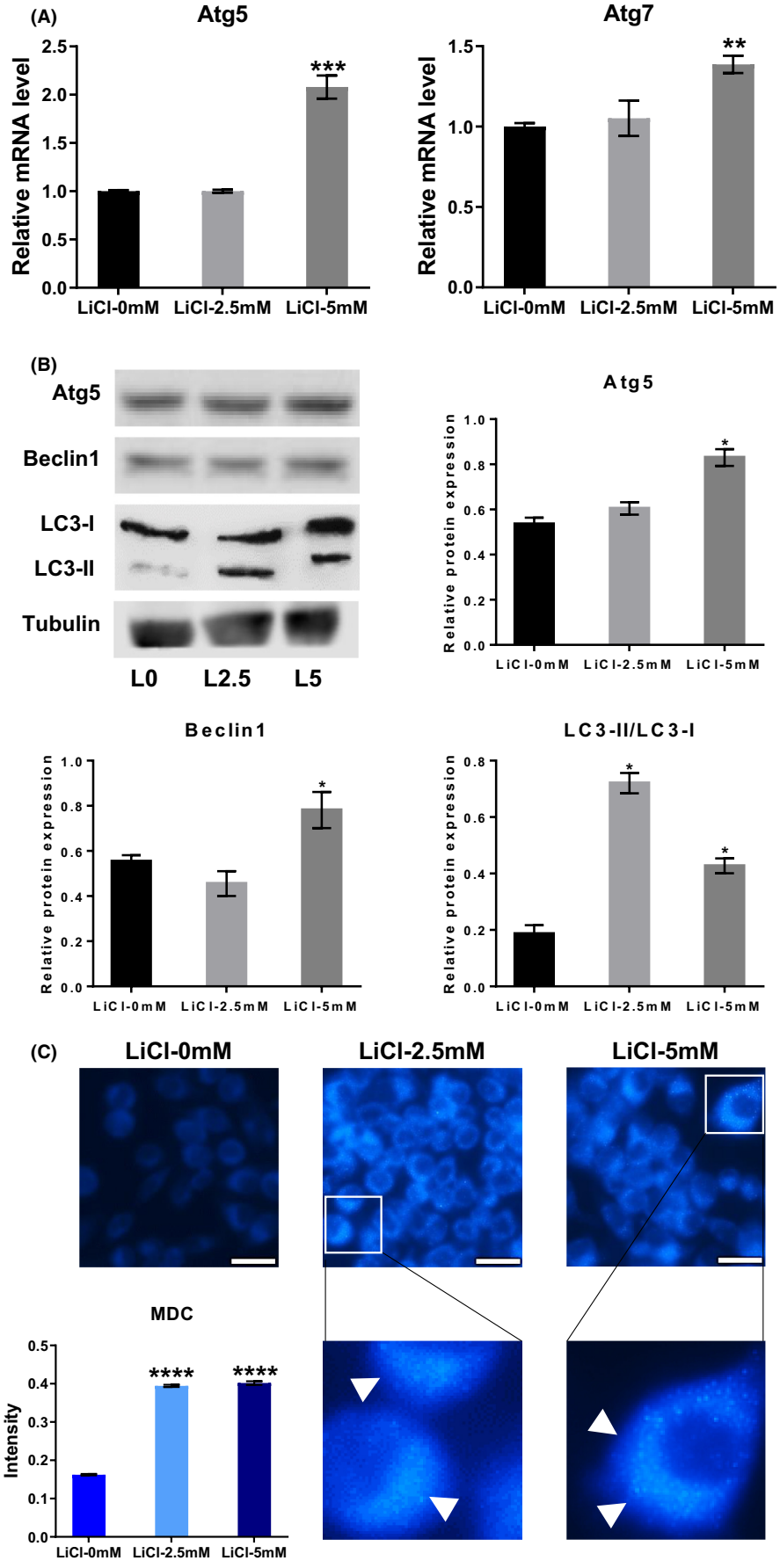

FIGURE 5 LiCl induced autophagic activity in macrophages. (A and B) LiCl treatment induced the mRNA and protein levels of essential autophagy markers. (C) LiCl application led to increased autophagosome formation in macrophages as indicated by MDC-positive sphere-like structures. Asterisk indicates significant difference (*$p < .05$; **$p < .01$; ***$p < .001$; ****$p < .0001$)

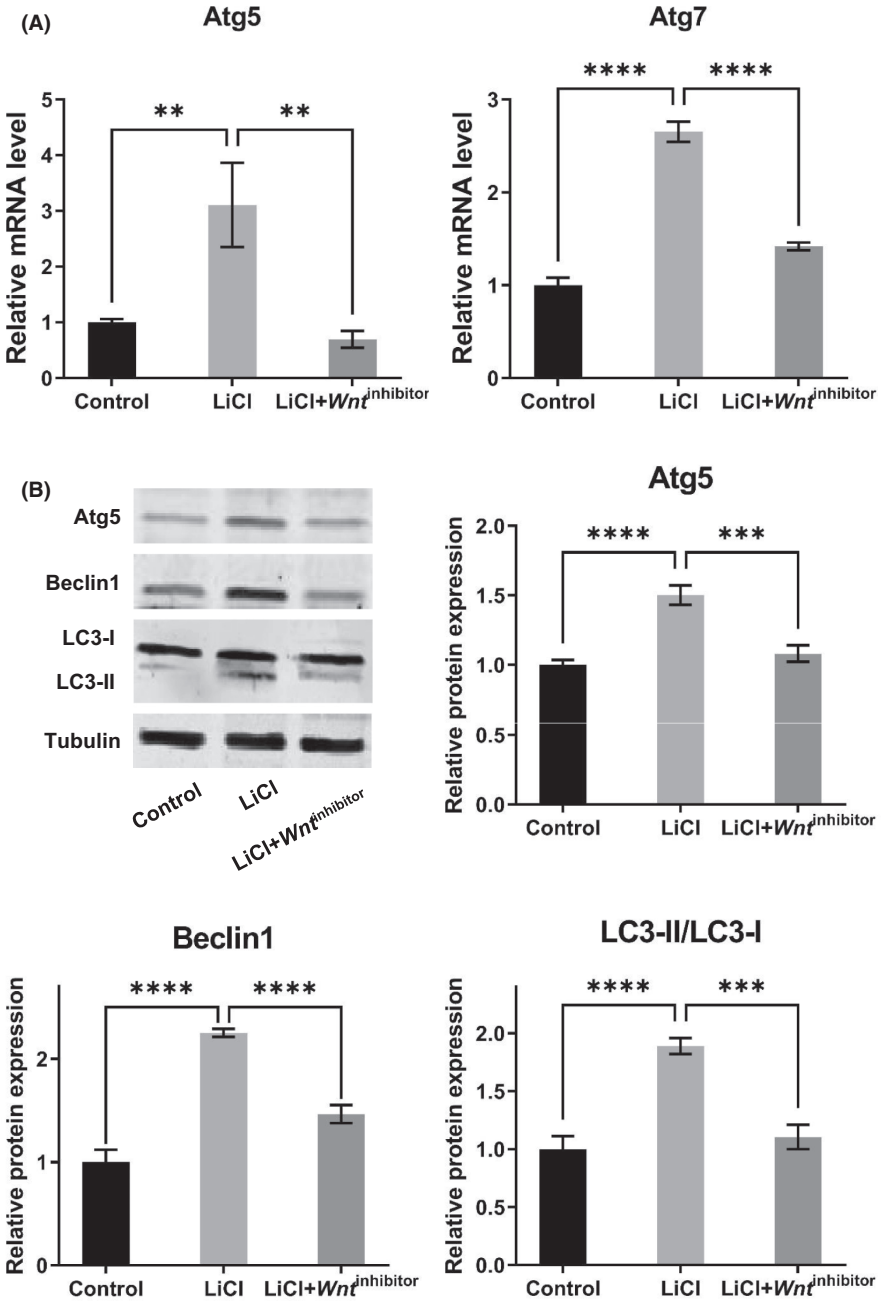

FIGURE 6 Application of Wnt inhibitor diminished the LiCl-induced autophagic activity as demonstrated in the significantly lower (A) mRNA and (B) protein expression levels of autophagy markers. Asterisk indicates significant difference (*$p < .05$; **$p < .01$; ***$p < .001$; ****$p < .0001$)

The available evidence suggests that activation of the Wnt/β-catenin pathway reduces several molecular inflammatory processes triggered by bacterial pathogens.[9,27] The fact that pro-inflammatory stimuli such as TNFα and IFNγ are able to increase the expression of Wnt/β-catenin signaling molecules indicates that these pathways are interconnected.[28,29] Pro-inflammatory stimulation by bacterial infections is likely to be a prerequisite to activate Wnt signaling, which means that Wnt/β-catenin activity is necessary for the late stages of inflammatory response.

The research presented here utilized the anti-inflammatory capacity of the Wnt/β-catenin signaling pathway, to establish a novel approach that regulates the pathological immune microenvironment in periodontal diseases. By using an animal model of periodontal defects, we observed the correlation between macrophage infiltration and β-catenin expression, suggesting Wnt/β-catenin signaling could be activated in the local macrophages for periodontal regeneration. We further applied LiCl to activate Wnt/β-catenin signaling and found significantly accelerated periodontal regeneration in the in vivo model, which induced a M1-to-M2 phenotype shift in macrophages within the periodontal defect area.

To demonstrate how LiCl-mediated Wnt/β-catenin signaling activation could mitigate inflammation and subsequently induce periodontal regeneration, LiCl was applied to stimulate macrophages in an inflammatory microenvironment in vitro. The results identify that Wnt/β-catenin signaling activation efficiently initiated the conversion of M1 (inflammatory) to M2 (tissue regenerative) macrophages, along with autophagy activation, which was in accordance with the previous findings that LiCl could suppress the

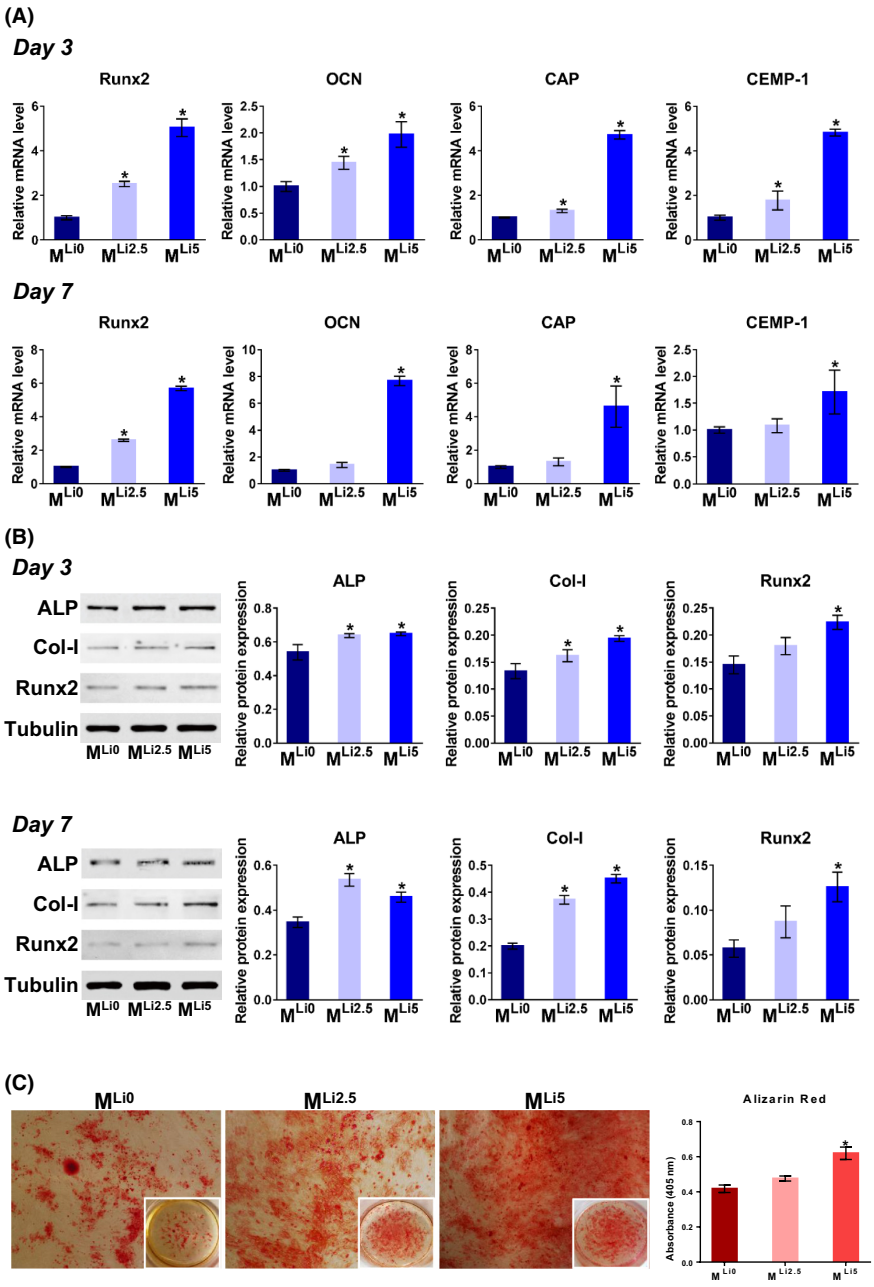

FIGURE 7 Li-activated macrophages mediated osteogenic/cementogenic differentiation of PDLCs. (A) RT-qPCR analysis showed upregulated gene expression levels of osteogenic markers (Runx2 and OCN) and cementogenic markers (CAP and CEMP1) in PDLCs on day 3 and day 7 of stimulation with conditioned medium derived from LiCl-activated macrophages. (B) Western blot analysis demonstrated a significant increase in osteogenic markers at the protein levels. (C) Alizarin Red S staining revealed significantly increased mineral depositions in PDLCs stimulated with conditioned medium derived from LiCl-activated macrophages in a dose-dependent manner. M^{Li0}, $M^{Li2.5}$, and M^{Li5}: conditioned medium derived from macrophages stimulated with LiCl at a concentration of 0, 2.5, and 5 mM, respectively. Asterisk indicates significant difference ($^*p < .05$)

inflammatory response and activate autophagy in monocytes.[15] As an indispensable homeostatic cellular process, autophagy has been reported to resolve macrophage inflammation by facilitating the clearance of reactive oxygen species,[30–35] which has been demonstrated to associate with M2 macrophage polarization, resulting in improved tissue regeneration as per our previous research.[36] The LiCl-induced M2 polarization presented here in this research could be partially achieved through the activation of autophagy, which should be further investigated in future. It also suggests that autophagy may serve as a target for immunomodulation to boost tissue regeneration. Inactivation of Wnt/β-catenin signaling using a commercially available Wnt inhibitor, on the contrary, could reverse the LiCl-mediated immunomodulatory effect. We further demonstrated that the LiCl treatment regulated macrophage response and eventually created an immune microenvironment beneficial for periodontal regeneration. This was supported by data showing that the pro-osteogenic cytokines such as BMP-2 and VEGF were upregulated in the conditioned medium derived from LiCl-treated macrophages, which could significantly facilitate the osteogenic/cementogenic differentiation of PDLCs, and induce cell mineralization, as compared to the controls.[12] These findings are consistent with a previously reported positive effect of Wnt signaling activation on cementum regeneration.[18]

Overall, these findings enhance the understanding of how LiCl-mediated Wnt/β-catenin signaling activation shapes the immune response. In addition, this study highlights unanswered questions, the solution of which will be imperative in the rational exploitation of the Wnt/β-catenin pathway in immunotherapy for periodontal diseases. Our study also provides a potential therapeutic target for periodontal regeneration, which could be utilized

to design and develop advanced biomedical materials/devices for translational application.

5 | CONCLUSION

LiCl activates Wnt/β-catenin signaling and modulates macrophage polarization from M1 to M2. LiCl-activated macrophages accelerate osteogenic and cementogenic differentiation of PDLCs. Targeting the Wnt/β-catenin pathway harnesses a unique combination of protective and regenerative approaches for the management of periodontal diseases.

ACKNOWLEDGEMENT

The authors declare that there is no conflict of interest. Funding for this study was provided by the National Health and Medical Research Council (NHMRC) Early Career Fellowship (Grant No. 1105035), the National Natural Science Foundation of China (NSFC) General Project (Grant No. 31771025), the NSFC Young Scientists Fund (Grant No. 81700969), and the Australian Dental Research Foundation Project (Grant No. 64-2016). Open access publishing facilitated by Queensland University of Technology, as part of the Wiley - Queensland University of Technology agreement via the Council of Australian University Librarians.

DATA AVAILABILITY STATEMENT

The data that support the findings of this study are available from the corresponding author upon reasonable request.

ORCID

Pingping Han https://orcid.org/0000-0001-7546-1635
Yinghong Zhou https://orcid.org/0000-0001-9757-7735

REFERENCES

1. Van Dyke TE, Sima C. Understanding resolution of inflammation in periodontal diseases: is chronic inflammatory periodontitis a failure to resolve? *Periodontology 2000*. 2020;82(1):205-213.
2. Mark Bartold P, Van Dyke TE. Host modulation: controlling the inflammation to control the infection. *Periodontology 2000*. 2017;75(1):317-329.
3. Hienz SA, Paliwal S, Ivanovski S. Mechanisms of bone resorption in periodontitis. *J Immunol Res*. 2015;2015:615486.
4. Cekici A, Kantarci A, Hasturk H, Van Dyke TE. Inflammatory and immune pathways in the pathogenesis of periodontal disease. *Periodontology 2000*. 2014;64(1):57-80.
5. Laskin DL. Macrophages and inflammatory mediators in chemical toxicity: a battle of forces. *Chem Res Toxicol*. 2009;22(8):1376-1385.
6. Steinhart Z, Angers S. Wnt signaling in development and tissue homeostasis. *Development*. 2018;145(11):1-8.
7. Ring A, Kim YM, Kahn M. Wnt/catenin signaling in adult stem cell physiology and disease. *Stem Cell Rev Rep*. 2014;10(4):512-525.
8. Chen L, Yang Y, Bao J, et al. Autophagy negative-regulating Wnt signaling enhanced inflammatory osteoclastogenesis from pre-OCs in vitro. *Biomed Pharmacother*. 2020;126:110093.
9. Silva-Garcia O, Valdez-Alarcon JJ, Baizabal-Aguirre VM. The Wnt/beta-catenin signaling pathway controls the inflammatory response in infections caused by pathogenic bacteria. *Mediators Inflamm*. 2014;2014:310183.
10. Xia MY, Zhao XY, Huang QL, et al. Activation of Wnt/beta-catenin signaling by lithium chloride attenuates d-galactose-induced neurodegeneration in the auditory cortex of a rat model of aging. *FEBS Open Biol*. 2017;7(6):759-776.
11. Hao H-P, Wen L-B, Li J-R, et al. LiCl inhibits PRRSV infection by enhancing Wnt/β-catenin pathway and suppressing inflammatory responses. *Antiviral Res*. 2015;117:99-109.
12. Yang C, Wang W, Zhu K, et al. Lithium chloride with immunomodulatory function for regulating titanium nanoparticle-stimulated inflammatory response and accelerating osteogenesis through suppression of MAPK signaling pathway. *Int J Nanomed*. 2019;14:7475-7488.
13. Yuan J, Hou Q, Chen D, et al. Chitosan/LiCl composite scaffolds promote skin regeneration in full-thickness loss. *Sci Chin Life Sci*. 2019;63:1-11.
14. Wang H-M, Zhang T, Li Q, Huang J-K, Chen R-F, Sun X-J. Inhibition of glycogen synthase kinase-3β by lithium chloride suppresses 6-hydroxydopamine-induced inflammatory response in primary cultured astrocytes. *Neurochem Int*. 2013;63(5):345-353.
15. Rahtes AA, Li LW. Reprogramming of inflammatory monocytes by autophagy modulator LiCl. *J Immunol*. 2017;198(1):70.
16. Li S, Shao J, Zhou Y, et al. The impact of Wnt signalling and hypoxia on osteogenic and cementogenic differentiation in human periodontal ligament cells. *Mol Med Rep*. 2016;14(6):4975-4982.
17. Zhou YH, Wu CT, Zhang XF, Han PP, Xiao Y. The ionic products from bredigite bioceramics induced cementogenic differentiation of periodontal ligament cells via activation of the Wnt/beta-catenin signalling pathway. *J Mater Chem B*. 2013;1(27):3380-3389.
18. Han P, Ivanovski S, Crawford R, Xiao Y. Activation of the canonical Wnt signaling pathway induces cementum regeneration. *J Bone Miner Res*. 2015;30(7):1160-1174.
19. Wong SK, Chin KY, Ima-Nirwana S. The skeletal-protecting action and mechanisms of action for mood-stabilizing drug lithium chloride: current evidence and future potential research areas. *Front Pharmacol*. 2020;11:430.
20. Atri C, Guerfali FZ, Laouini D. Role of human macrophage polarization in inflammation during infectious diseases. *Int J Mol Sci*. 2018;19(6):1-15.
21. Ivanovski S. Periodontal regeneration. *Aust Dent J*. 2009;54(Suppl 1):S118-S128.
22. Silva N, Abusleme L, Bravo D, et al. Host response mechanisms in periodontal diseases. *J Appl Oral Sci*. 2015;23(3):329-355.
23. Swafford D, Manicassamy S. Wnt signaling in dendritic cells: its role in regulation of immunity and tolerance. *Discov Med*. 2015;19(105):303-310.
24. MacDonald BT, He X. Frizzled and LRP5/6 receptors for Wnt/beta-catenin signaling. *Cold Spring Harb Perspect Biol*. 2012;4(12):1-24.
25. MacDonald BT, Tamai K, He X. Wnt/beta-catenin signaling: components, mechanisms, and diseases. *Dev Cell*. 2009;17(1):9-26.
26. Lovatt M, Bijlmakers MJ. Stabilisation of beta-catenin downstream of T cell receptor signalling. *PLoS One*. 2010;5(9):e12794.
27. Li D, Wang W, Wu Y, Ma X, Zhou W, Lai Y. Lipopeptide 78 from *Staphylococcus epidermidis* activates beta-catenin to inhibit skin inflammation. *J Immunol*. 2019;202(4):1219-1228.
28. Li D, Beisswenger C, Herr C, et al. Myeloid cell RelA/p65 promotes lung cancer proliferation through Wnt/beta-catenin signaling in murine and human tumor cells. *Oncogene*. 2014;33(10):1239-1248.
29. Yuan XL, He F, Zheng FX, Xu YL, Zou JT. Interferon-gamma facilitates neurogenesis by activating Wnt/beta-catenin cell signaling pathway via promotion of STAT1 regulation of the beta-catenin promoter (vol 448, pg 219, 2020). *Neuroscience*. 2021;459:198.

30. Zhong Z, Umemura A, Sanchez-Lopez E, et al. NF-κB restricts inflammasome activation via elimination of damaged mitochondria. *Cell*. 2016;164(5):896-910.
31. Shi J, Wong J, Piesik P, et al. Cleavage of sequestosome 1/p62 by an enteroviral protease results in disrupted selective autophagy and impaired NFKB signaling. *Autophagy*. 2013;9(10):1591-1603.
32. Zhong Z, Sanchez-Lopez E, Karin M. Autophagy, inflammation, and immunity: a troika governing cancer and its treatment. *Cell*. 2016;166(2):288-298.
33. Elliott EI, Sutterwala FS. Initiation and perpetuation of NLRP 3 inflammasome activation and assembly. *Immunol Rev*. 2015;265(1):35-52.
34. Zhou R, Yazdi AS, Menu P, Tschopp J. A role for mitochondria in NLRP3 inflammasome activation. *Nature*. 2011;469(7329):221-225.
35. Qian S, Fan J, Billiar TR, Scott MJ. Inflammasome and autophagy regulation: a two-way street. *Mol Med*. 2017;23:188.
36. Xiao L, Wei F, Zhou Y, et al. Dihydrolipoic acid–gold nanoclusters regulate microglial polarization and have the potential to alter neurogenesis. *Nano Letters*. 2019;20(1):478-495.

SUPPORTING INFORMATION

Additional supporting information may be found in the online version of the article at the publisher's website.

How to cite this article: Zheng X, Wang S, Xiao L, et al.. LiCl-induced immunomodulatory periodontal regeneration via the activation of the Wnt/β-catenin signaling pathway. *J Periodont Res*. 2022;57:835-848. doi: 10.1111/jre.13022